JOURNAL OF SYNCHROTRON RADIATION

ISSN 1600-5775

# Iterative energy self-calibration of Fe XANES spectra. Erratum

Michael W. M. Jones,[a]* Guilherme Mallmann,[b] Jeremy L. Wykes,[c] Joseph Knafelc,[d] Scott E. Bryan[d] and Daryl L. Howard[c]

[a]Institute for Future Environments, Central Analytical Research Facility, Queensland University of Technology, Brisbane, Australia, [b]Research School of Earth Sciences, Australian National University, Canberra, Australia, [c]ANSTO Australian Synchrotron, Clayton, Australia, and [d]School of Earth, Environmental and Biological Sciences, Queensland University of Technology, Brisbane, Australia. *Correspondence e-mail: mw.jones@qut.edu.au

Received 19 June 2020
Accepted 19 June 2020

Edited by R. W. Strange, University of Essex, UK

**Keywords:** Fe XANES; energy calibration; mid-ocean ridge basalt (MORB); RGM-2; rhyolite; Havre pumice

A correction is made to the paper by Jones *et al.* (2020). [*J. Synchrotron Rad.* **27**, 207–211].

In the paper by Jones *et al.* (2020), the authors have noted that an incorrect value was published for the calibrated $Fe^{3+}/\Sigma Fe$ for the rafted pumice sample from the 2012 Havre eruption. The correct value is 0.257 (0.010) and is included in the updated Table 2 below and updated in the inset in Fig. 3(*c*) (overleaf).

**Table 2**
Summary of uncalibrated and self-calibrated values for the data presented in Fig. 3, where the uncalibrated, self-calibrated and expected $Fe^{3+}/\Sigma Fe$ ratios are presented together with the required energy change ($\Delta E$).

| | $Fe^{3+}/\Sigma Fe$ | | | |
|---|---|---|---|---|
| Sample | Uncalibrated | Self-calibrated | Expected | $\Delta E$ (eV) |
| MORB VG 3450 | 0.591 (0.018) | 0.129 (0.004) | 0.132 | 0.8 |
| RGM-2 | 0.535 (0.037)† | 0.231 (0.016) | 0.262 (0.015)‡ | 0.3§ |
| Havre pumice | 0.452 (0.031)† | 0.257 (0.010) | — | 0.5§ |

† Manually offset to be within calibration range. ‡ RGM-1 values. § After manual offset.

## References

Berry, A. J., Stewart, G. A., O'Neill, H. St C., Mallmann, G. & Mosselmans, J. F. W. (2018). *Earth Planet. Sci. Lett.* **483**, 114–123.
Cottrell, E., Kelley, K. A., Lanzirotti, A. & Fischer, R. A. (2009). *Chem. Geol.* **268**, 167–179.
Jones, M. W. M., Mallmann, G., Wykes, J. L., Knafelc, J., Bryan, S. E. & Howard, D. L. (2020). *J. Synchrotron Rad.* **27**, 207–211.

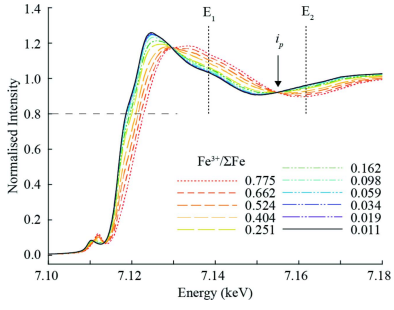

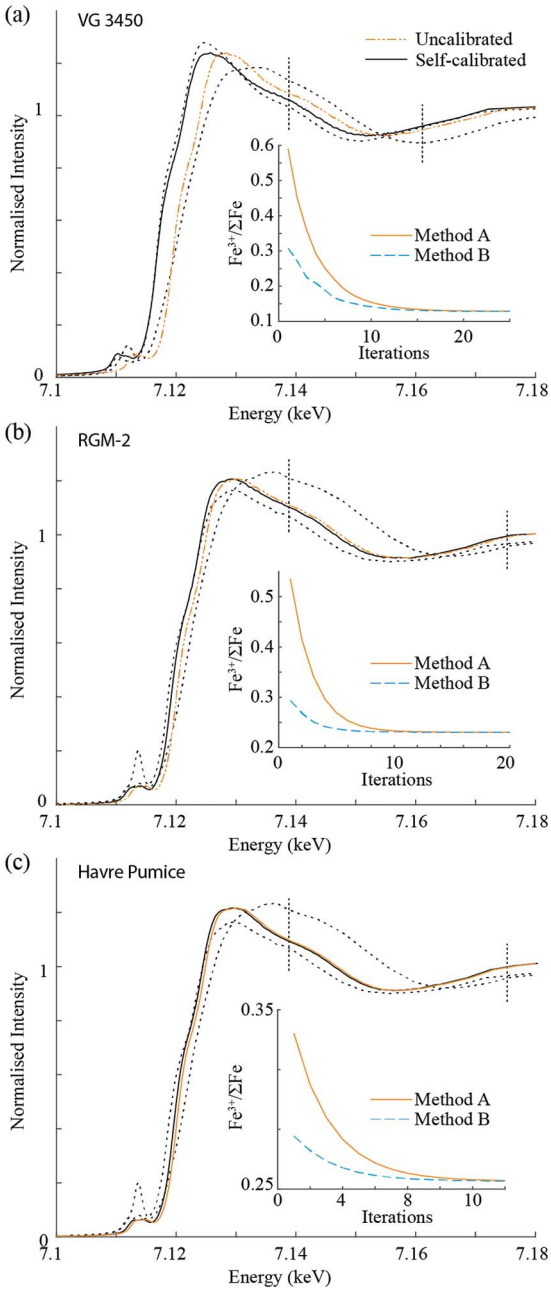


**Figure 3**
Demonstration of iterative energy calibration correction. (*a*) A MORB glass spectra (Smithsonian Institute sample number VG 3450), as collected by Berry *et al.* (2018) (orange dot–dashed line), iteratively self-corrected (solid black line) to the basaltic glass standards. Also shown for reference are the spectra for the 0.011 and 0.775 $Fe^{3+}/\Sigma Fe$ ratio standards (black dotted lines). The $Fe^{3+}/\Sigma Fe$ ratio (inset) for Method A (solid orange lines) and B (dashed blue lines) as a function of iteration number shows convergence to a single $Fe^{3+}/\Sigma Fe$ ratio. Similar treatment is shown for the RGM-2 reference standard (*b*) and an experimental section of pumice from the 2012 Havre eruption (*c*), both iteratively self-corrected to the rhyolite glass standards (Cottrell *et al.*, 2009). Also shown for reference are the spectra for the 0.238 and 0.806 $Fe^{3+}/\Sigma Fe$ ratio standards (black dotted lines). The vertical dashed lines in (*a*)–(*c*) refer to the two points $E_1$ and $E_2$ in each case.

JOURNAL OF SYNCHROTRON RADIATION

ISSN 1600-5775

Received 12 August 2019
Accepted 18 October 2019

Edited by R. W. Strange, University of Essex, UK

**Keywords:** Fe XANES; energy calibration; mid-ocean ridge basalt (MORB); RGM-2; rhyolite; Havre pumice.

**Supporting information**: this article has supporting information at journals.iucr.org/s

# Iterative energy self-calibration of Fe XANES spectra

**Michael W. M. Jones,[a]* Guilherme Mallmann,[b] Jeremy L. Wykes,[c] Joseph Knafelc,[d] Scott E. Bryan[d] and Daryl L. Howard[c]**

[a]Institute for Future Environments, Central Analytical Research Facility, Queensland University of Technology, Brisbane, Australia, [b]Research School of Earth Sciences, Australian National University, Canberra, Australia, [c]ANSTO Australian Synchrotron, Clayton, Australia, and [d]School of Earth, Environmental and Biological Sciences, Queensland University of Technology, Brisbane, Australia. *Correspondence e-mail: mw.jones@qut.edu.au

Determining the oxidation state of Fe through parameterization of X-ray absorption near-edge structure (XANES) spectral features is highly dependent on accurate and repeatable energy calibration between spectra. Small errors in energy calibration can lead to vastly different interpretations. While simultaneous measurement of a reference foil is often undertaken on X-ray spectroscopy beamlines, other beamlines measure XANES spectra without a reference foil and therefore lack a method for correcting energy drift. Here a method is proposed that combines two measures of Fe oxidation state taken from different parts of the spectrum to iteratively correct for an unknown energy offset between spectra, showing successful iterative self-calibration not only during individual beam time but also across different beamlines.

## 1. Introduction

Iron is an abundant element with critical importance to many aspects of our lives, from steelmaking to the formation of red blood cells. Fe usually occurs in oxidized form, either as $Fe^{2+}$ (ferrous iron) or $Fe^{3+}$ (ferric iron), each with distinct chemical properties. The reaction involving reduction or oxidation of Fe is a fundamental process (Ilbert & Bonnefoy, 2013; McCammon, 2005; Potapkin *et al.*, 2013; O'Neill *et al.*, 2018) and quantifying the direction and extent of this reaction is a major goal in science.

Fe *K*-edge X-ray absorption near-edge structure (XANES) has become the method of choice for quantitative determination of Fe oxidation state, expressed as the concentration ratio $Fe^{3+}/\Sigma Fe$ where $\Sigma Fe = Fe^{2+} + Fe^{3+}$, via empirical fitting of unknowns to a calibration curve developed from a suite of standards with independently determined $Fe^{3+}/\Sigma Fe$ ratios. An Fe *K*-edge XANES spectrum can be parameterized via a number of methods, such as the centroid energy of the combined pre-edge peaks (Fiege *et al.*, 2017; Berry *et al.*, 2018, 2003; Cottrell *et al.*, 2009; Dyar *et al.*, 2012), the energy of a specific normalized intensity along the absorption edge (Berry *et al.*, 2018; Nedoseykina *et al.*, 2010; Dyar *et al.*, 2012) or the ratio of normalized intensities at two post-edge energies (Berry *et al.*, 2010; Dyar *et al.*, 2012). The relationship between any of these points and the known $Fe^{3+}/\Sigma Fe$ ratio of standards can be fitted, allowing the $Fe^{3+}/\Sigma Fe$ ratio of an unknown specimen to be easily determined provided the composition and structure of standards and unknowns are similar; criteria easily satisfied by using synthetic glass standards. However, any error in the energy calibration feeds directly into the $Fe^{3+}/\Sigma Fe$ quantification making empirical methods extremely

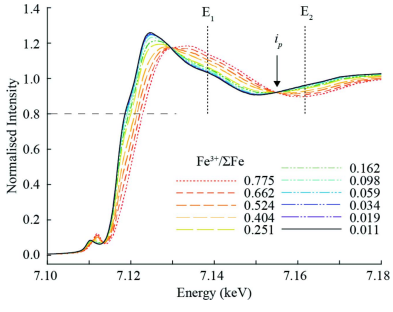

**Table 1**
Samples used in the present study.

| Sample | $Fe^{3+}/\Sigma Fe$ | Beamline (facility) |
|---|---|---|
| 11 × Basalt standards† | 0.011–0.775†‡ | XFM (AS)§ |
| 7 × Rhyolite standards¶ | 0.238–0.806‡†† | X26A (NSLS)¶ |
| MORB VG 3450† | 0.132†‡‡ | I18 (Diamond) |
| RGM-2§§ | 0.262¶¶ | XFM (AS)§ |
| Havre pumice††† | Unknown | XFM (AS)§ |

† As described by Berry *et al.* (2018). ‡ Determined by Mössbauer spectroscopy. § This study. ¶ As described by Cottrell *et al.* (2009). †† Determined by wet chemistry. ‡‡ Determined by XANES. §§ USGS natural rhyolite standard. ¶¶ Values determined from USGS natural rhyolite standard RGM-1. ††† Sea-rafted rhyolitic pumice from the 2012 Havre eruption (Carey *et al.*, 2018).

sensitive to the scan-to-scan energy reproducibility. For example, the entire range of $Fe^{3+}/\Sigma Fe$ from 0 to 1 in silicate glasses of basaltic composition results in a change of <6 eV in the absorption edge at a normalized intensity of 0.8 and an even smaller change of <2 eV in the pre-edge centroid (Fiege *et al.*, 2017; Berry *et al.*, 2018). The resolution and reproducibility of monochromators are therefore critical in making precise determinations of $Fe^{3+}/\Sigma Fe$.

At beamlines employing double-crystal monochromators, time-dependent changes in the relationship between the nominal incident energy and the true incident energy, herein termed energy drift, typically arise because of changes in the geometric relationship between the Bragg axis encoder and the lattice planes of the diffracting crystals. Energy drift is highly dependent on a combination of factors, including monochromator mechanical design, thermal management and storage-ring top-up frequency.

A typical method to correct energy drift and perform an absolute energy calibration during $Fe^{3+}/\Sigma Fe$ determinations is to simultaneously collect the spectrum of an Fe foil. The Fe foil spectrum can then be calibrated by using the energy of the first derivative peak (Fiege *et al.*, 2017) for example, with the calibration factor then applied to the simultaneously collected unknown spectra. However, in some cases this approach is impractical, either because of a specific experimental setup [*e.g.* simultaneously collecting ptychography data using the transmitted beam (Jones *et al.*, 2016)] or because of beamline design [*e.g.* the X-ray Fluorescence Microscopy (XFM) beamline at the Australian Synchrotron (AS) (Paterson *et al.*, 2011), which lacks the ability to simultaneously measure a reference standard]. Additionally, there may be occasions where reference foils were collected at intervals insufficient to develop a time-dependent expression for energy drift and, therefore, an alternate method is necessary to salvage the dataset.

Silicate melts, quenched to glass, are sensitive recorders of magmatic $Fe^{3+}/\Sigma Fe$ and thus capture the oxygen fugacity of magmatic systems on eruption. The accurate quantitative determination of $Fe^{3+}/\Sigma Fe$ in natural silicate glasses is essential in studying these systems, with uncertainty in the energy calibration potentially rendering an entire beam time dedicated to Fe *K*-edge XANES analysis worthless.

Here, we develop a method of iterative self-calibration of Fe XANES spectra that combines information from both the rising edge and the post-edge structure, allowing precise energy calibration of unknown spectra without a simultaneously measured reference foil. Furthermore, we apply this method to iteratively self-calibrate spectra between beamlines, opening the possibility for all researchers to use a single set of high-quality calibration standards for each system being investigated, making data collection more efficient and direct comparisons between beam times trivial.

## 2. Method

### 2.1. Sample description

The samples used were a mix of synthetic and natural samples collected at a variety of beamlines. Table 1 provides a summary of the samples used in this study.

### 2.2. Data collection

Fe *K*-edge XANES data for this study were collected at the XFM beamline at the AS (Paterson *et al.*, 2011) at 220 energies between 6.963 keV and 7.462 keV with non-uniform energy spacing (see Table S2 in the supporting information). For each of the 11 synthetic glass standards and the rhyolite RGM-2 standard, 200 individual pixel-wise spectra were collected with 10 ms per energy yielding an equivalent dwell of 2 s per energy across the sample. Similarly, the pumice sample was collected with a dwell of ∼32 s per energy. Excited fluorescent photons from a 2 µm full width at half-maximumX-ray focus formed by a Kirkpatrick–Baez mirror pair were collected using a Maia (Rev D) detector system positioned in its typical backscatter geometry (Siddons *et al.*, 2014; Ryan *et al.*, 2018). Fluorescent data were analysed using the dynamic analysis method (Ryan & Jamieson, 1993) implemented in *GeoPIXE* (Ryan *et al.*, 2005) and quantified using known metallic foils (Micromatter, Canada). The Fe maps for each incident energy were exported as quantitative TIFF files yielding pixel-wise XANES spectra for each sample. All spectra had a constant pre-edge background subtracted and were normalized to an edge step of 1.

### 2.3. Iterative self-calibration

We generated two parameterizations of the relationship between spectral features of the standards and their independently determined $Fe^{3+}/\Sigma Fe$ ratios for both the basalt and rhyolite glass standards. Method A involved determining the energy where the absorption edge reaches a normalized intensity of 0.8, while Method B involved determining the ratio of the normalized intensity of two post-edge energies ($E_1$ and $E_2$), with linear fits performed for each method against $Fe^{3+}/\Sigma Fe$. While the values (0.8, $E_1$ and $E_2$) are somewhat arbitrary, they were chosen to obtain maximum energy or intensity separation while maintaining a linear relationship to $Fe^{3+}/\Sigma Fe$ concentration. $E_1$ and $E_2$ were taken as 7138.4 eV and 7161.7 eV, respectively, for the basalts as previously described by Berry *et al.* (2018), while $E_2$ was extended to 7175 eV for the rhyolites because of the poorly defined isosbestic point for the natural standards. The normalized

spectra and the fits to both Methods A and B are shown in Figs. 1 and 2 for basaltic and rhyolite glasses, respectively. We note that the error bars in Fig. 1(*b*) are one standard deviation from the 200 individual measurements (this study), whereas in Fig. 2(*b*) the error bars indicate the extent of variability from the three individual measurements (Cottrell *et al.*, 2009).

Two methods are needed in tandem to constrain the energy calibration to a single solution. For example, a spectrum offset to lower energy will result in an under-reporting of the $Fe^{3+}/\Sigma Fe$ concentration using Method A (edge moves to lower energy) and an over-reporting of the $Fe^{3+}/\Sigma Fe$ concentration using Method B ($I_2/I_1$ increases as the spectrum shifts to the left). However, we can combine these two methods to adjust the energy offset in an iterative process converging on a single value for the $Fe^{3+}/\Sigma Fe$ concentration,

$$\lim_{\Delta E \to 0} E + \Delta E = E_c,$$

where $E$ is the energy scale and $E_c$ is the final self-calibrated energy scale. $\Delta E = E_A(\overline{Fe_{AB}}) - E_A(Fe_A)$, where $Fe_A$ is the $Fe^{3+}/\Sigma Fe$ ratio using Method A, $\overline{Fe_{AB}}$ is the mean $Fe^{3+}/\Sigma Fe$ ratio using Methods A and B, and $E_A(\overline{Fe_{AB}})$ is the energy of the edge given the $Fe^{3+}/\Sigma Fe$ ratio $\overline{Fe_{AB}}$. In the present case the iterative process was stopped when $\Delta E < 10^{-4}$ eV. At this point, both methods report the same value for the $Fe^{3+}/\Sigma Fe$ ratio and the energy, and therefore the $Fe^{3+}/\Sigma Fe$ ratio, is calibrated.

We apply this method to three cases. Firstly, to a mid-ocean-ridge basalt (MORB) sample (VG 3450) spectra with a previously determined $Fe^{3+}/\Sigma Fe$ ratio (Berry *et al.*, 2018) using the basaltic glass standard reference spectra. Secondly, to a thin section of the USGS rhyolite standard RGM-2, and thirdly, to a thin section of rhyolitic pumice collected at the XFM beamline at the AS using the rhyolite glass standard

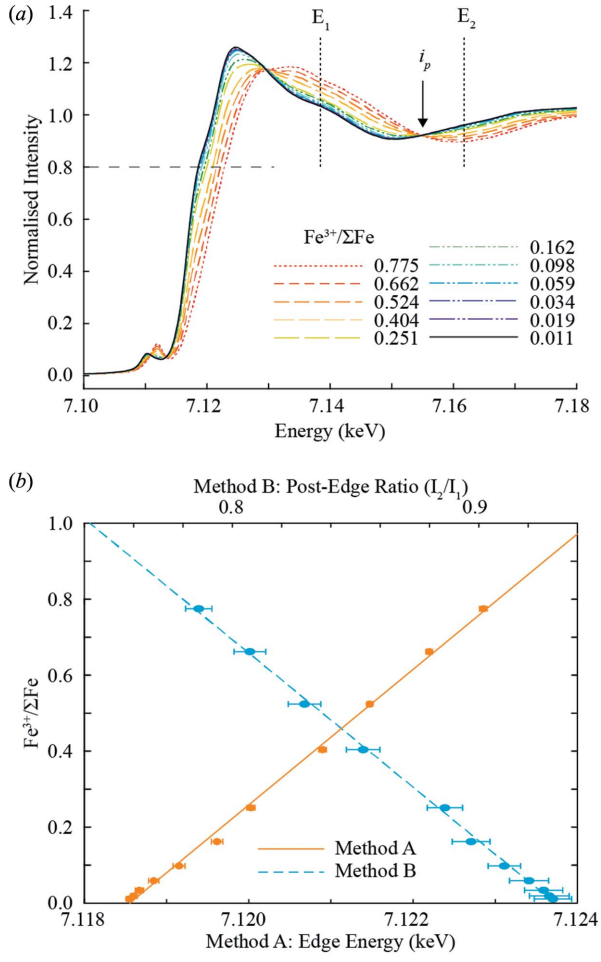


**Figure 1**
(*a*) Fe-XANES spectra from 11 synthetic basalt standards with $Fe^{3+}/\Sigma Fe$ between 0.011 and 0.775. The horizontal dashed line represents a normalized intensity of 0.8 (Method A) and the vertical dashed lines correspond to the points $E_1$ = 7138.4 eV and $E_2$ = 7161.7 eV, placed either side of the isosbestic point $i_p$, with the ratio of the normalized intensity at $E_1$ and $E_2$ used to determine the $Fe^{3+}/\Sigma Fe$ concentration (Method B). (*b*) Results from Method A (orange solid line, lower axis) and Method B (blue dashed line, upper axis), where the error bars represent one standard deviation, calculated from the 200 individual measurements.

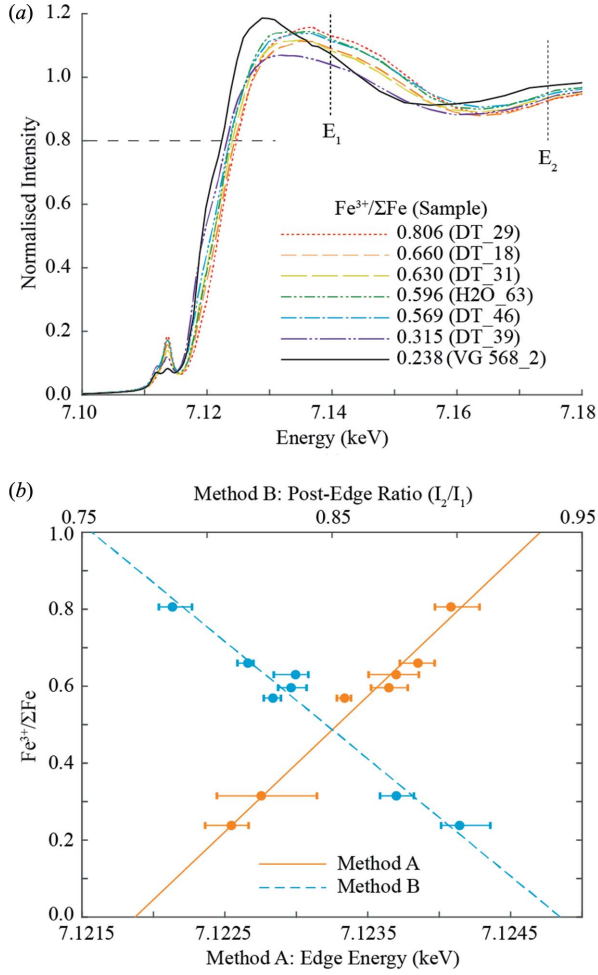


**Figure 2**
(*a*) Fe-XANES spectra from seven rhyolite standards with $Fe^{3+}/\Sigma Fe$ between 0.238 and 0.805 (Cottrell *et al.*, 2009). The horizontal dashed line represents a normalized intensity of 0.8 (Method A) and the vertical dashed lines correspond to the points $E_1$ = 7138.4 eV and $E_2$ = 7175.0 eV, with the ratio of the normalized intensity at $E_1$ and $E_2$ used to determine the $Fe^{3+}/\Sigma Fe$ concentration (Method B). (*b*) Results from Method A (orange solid line, lower axis) and Method B (blue dashed line, upper axis). The error bars in (*b*) represent the limits of the range from three measurements (Cottrell *et al.*, 2009).

**Table 2**
Summary of uncalibrated and self-calibrated values for the data presented in Fig. 2, where the uncalibrated, self-calibrated and expected $Fe^{3+}/\Sigma Fe$ ratios are presented together with the required energy change ($\Delta E$).

| | $Fe^{3+}/\Sigma Fe$ | | | |
|---|---|---|---|---|
| Sample | Uncalibrated | Self-calibrated | Expected | $\Delta E$ (eV) |
| MORB VG 3450 | 0.591 (0.018) | 0.129 (0.004) | 0.132 | 0.8 |
| RGM-2 | 0.535 (0.037)† | 0.231 (0.016) | 0.262 (0.015)‡ | 0.3§ |
| Havre pumice | 0.452 (0.031)† | 0.149 (0.010) | — | 0.4§ |

† Manually offset to be within calibration range. ‡ RGM-1 values. § After manual offset.

reference spectra (Cottrell *et al.*, 2009). Further details and an example *Matlab* code are presented in the supporting information.

## 3. Results and discussion

The results for the MORB sample, RGM-2 and the Havre raft pumice are presented in Figs. 3(*a*)–3(*c*), respectively. Here we observe that the proposed method of energy self-calibration successfully converges on the correct $Fe^{3+}/\Sigma Fe$ ratio for the MORB sample, converging to a $Fe^{3+}/\Sigma Fe$ concentration of 0.129 [Fig. 3(*a*)]. In addition, we observe that the self-calibration method can also be successfully applied to rhyolite samples, with the RGM-2 sample converging to a $Fe^{3+}/\Sigma Fe$ ratio of 0.231 [Fig. 3(*b*)] and the previously unknown Havre pumice sample converging to a $Fe^{3+}/\Sigma Fe$ ratio of 0.149 [Fig. 3(*c*)]. A summary of the results is presented in Table 2.

We have shown that the proposed method can accurately correct an unknown energy offset in Fe XANES data of isotropic non-crystalline materials. Furthermore, we have shown that the current method can not only be used for correcting an energy drift during a beam time but also for correcting discrepancies in the absolute energy calibration between multiple beam times or indeed between multiple beamlines, as highlighted by the successful calibration of the MORB spectra, where we identify an absolute energy offset of 0.8 eV between two independent beam times at beamlines I18 at the Diamond Light Source and XFM at the AS. In addition, we determine the calibrated value for the $Fe^{3+}/\Sigma Fe$ ratio of the USGS RGM-2 standard sample to be 0.231 using a set of rhyolite standards. This represents the first estimation of $Fe^{3+}/\Sigma Fe$ ratio for this new standard material that has been collected from the same locality as the previous block of rhyolite standard RGM-1 (Wilson, 2019).

Furthermore, we apply the method to a sample of sea-rafted rhyolitic pumice from the 2012 Havre eruption (Carey *et al.*, 2018). We obtain a value for the $Fe^{3+}/\Sigma Fe$ ratio of 0.149, the first reported value for pumice from this significant unobserved submarine eruption. Establishing the oxidation state and magmatic $Fe^{3+}/\Sigma Fe$ ratio is often difficult for such crystal-poor rhyolites because of the lack of co-existing oxide minerals that are typically used to constrain oxygen fugacity of the magmatic system on eruption (*e.g.* Buddington & Lindsley, 1964; Ghiorso & Evans, 2008).

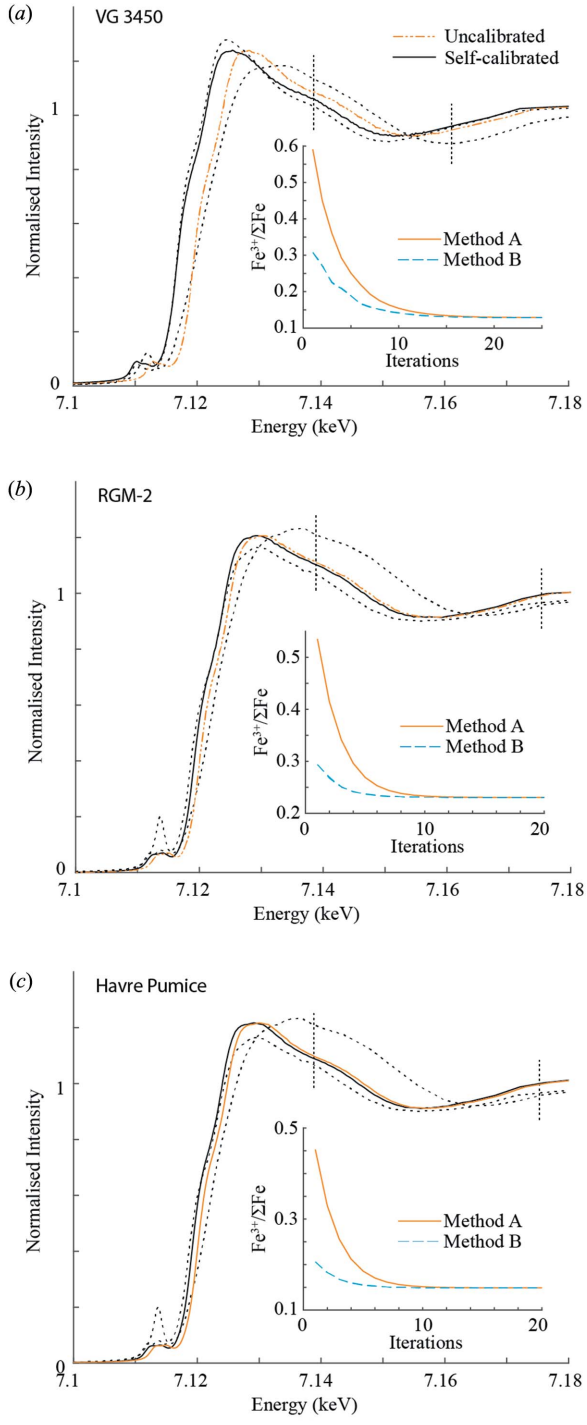


**Figure 3**
Demonstration of iterative energy calibration correction. (*a*) A MORB glass spectra (Smithsonian Institute sample number VG 3450), as collected by Berry *et al.* (2018) (orange dot–dashed line), iteratively self-corrected (solid black line) to the basaltic glass standards. Also shown for reference are the spectra for the 0.011 and 0.775 $Fe^{3+}/\Sigma Fe$ ratio standards (black dotted lines). The $Fe^{3+}/\Sigma Fe$ ratio (inset) for Method A (solid orange lines) and B (dashed blue lines) as a function of iteration number shows convergence to a single $Fe^{3+}/\Sigma Fe$ ratio. Similar treatment is shown for the RGM-2 reference standard (*b*) and an experimental section of pumice from the 2012 Havre eruption (*c*), both iteratively self-corrected to the rhyolite glass standards (Cottrell *et al.*, 2009). Also shown for reference are the spectra for the 0.238 and 0.806 $Fe^{3+}/\Sigma Fe$ ratio standards (black dotted lines). The vertical dashed lines in (*a*)–(*c*) refer to the two points $E_1$ and $E_2$ in each case.

The ability to calibrate unknown samples to a set of reference spectra collected at a different time and place potentially allows for a single set of absolute reference spectra to be collected and used by researchers to calibrate their unknowns. This would not only allow results to be easily compared but could also remove the need to collect a set of reference spectra at every beam time, saving multiple hours of costly beam time and allowing additional unknown samples to be studied. The proposed method can in theory be used to correct any spectra from isotropic non-crystalline materials where two opposing oxidation-dependent trends can be identified, such as the rising edge energy, the intensity or energy of pre-edge features, or the ratio of the intensity of pre- or post-edge features, provided the same method is used for the known and unknown samples and each sample type is compositionally similar.

## Acknowledgements

This research was undertaken on the XFM beamline at the Australian Synchrotron, part of ANSTO. We would like to thank Dr Andrew Berry (Australian National University) for providing MORB glass spectra collected at the Diamond Light Source beamline I18 and Dr Elizabeth Cottrell (Smithsonian Institution) for providing rhyolite glass reference spectra collected at the National Synchrotron Light Source (NSLS) beamline X26A. Stephen Wilson (USGS) is also thanked for providing samples of the Glass Mountain Rhyolite standard.

## Funding information

GM acknowledges support from the Australian Research Council (DE160100169). JK would like to thank AINSE Limited for providing financial assistance (Award-PGRA) to enable work on the XFM beamline at the Australian Synchrotron.

## References

Berry, A. J., O'Neill, H. St C., Jayasuriya, K. D., Campbell, S. J. & Foran, G. J. (2003). *Am. Mineral.* **88**, 967–977.
Berry, A. J., Stewart, G. A., O'Neill, H. St C., Mallmann, G. & Mosselmans, J. F. W. (2018). *Earth Planet. Sci. Lett.* **483**, 114–123.
Berry, A. J., Yaxley, G. M., Woodland, A. B. & Foran, G. J. (2010). *Chem. Geol.* **278**, 31–37.
Buddington, A. F. & Lindsley, D. H. (1964). *J. Petrol.* **5**, 310–357.
Carey, R., Soule, S. A., Manga, M., White, J. D. L., McPhie, J., Wysoczanski, R., Jutzeler, M., Tani, K., Yoerger, D., Fornari, D., Caratori-Tontini, F., Houghton, B., Mitchell, S., Ikegami, F., Conway, C., Murch, A., Fauria, K., Jones, M., Cahalan, R. & McKenzie, W. (2018). *Sci. Adv.* **4**, e1701121.
Cottrell, E., Kelley, K. A., Lanzirotti, A. & Fischer, R. A. (2009). *Chem. Geol.* **268**, 167–179.
Dyar, M. D., Breves, E. A., Emerson, E., Bell, S. W., Nelms, M., Ozanne, M. V., Peel, S. E., Carmosino, M. L., Tucker, J. M., Gunter, M. E., Delaney, J. S., Lanzirotti, A. & Woodland, A. B. (2012). *Am. Mineral.* **97**, 1726–1740.
Fiege, A., Ruprecht, P., Simon, A. C., Bell, A. S., Göttlicher, J., Newville, M., Lanzirotti, T. & Moore, G. (2017). *Am. Mineral.* **102**, 369–380.
Ghiorso, M. S. & Evans, B. W. (2008). *Am. J. Sci.* **308**, 957–1039.
Ilbert, M. & Bonnefoy, V. (2013). *Biochim. Biophys. Acta*, **1827**, 161–175.
Jones, M. W. M., Phillips, N. W., van Riessen, G. A., Abbey, B., Vine, D. J., Nashed, Y. S. G., Mudie, S. T., Afshar, N., Kirkham, R., Chen, B., Balaur, E. & de Jonge, M. D. (2016). *J. Synchrotron Rad.* **23**, 1151–1157.
McCammon, C. (2005). *Science*, **308**, 807–808.
Nedoseykina, T., Kim, M. G., Park, S.-A., Kim, H.-S., Kim, S.-B., Cho, J. & Lee, Y. (2010). *Electrochim. Acta*, **55**, 8876–8882.
O'Neill, H. S. C., Berry, A. J. & Mallmann, G. (2018). *Earth Planet. Sci. Lett.* **504**, 152–162.
Paterson, D., de Jonge, M. D., Howard, D. L., Lewis, W., McKinlay, J., Starritt, A., Kusel, M., Ryan, C. G., Kirkham, R., Moorhead, G., Siddons, D. P., McNulty, I., Eyberger, C. & Lai, B. (2011). *AIP Conf. Proc.* **1365**, 219–222.
Potapkin, V., McCammon, C., Glazyrin, K., Kantor, A., Kupenko, I., Prescher, C., Sinmyo, R., Smirnov, G. V., Chumakov, A. I., Rüffer, R. & Dubrovinsky, L. (2013). *Nat. Commun.* **4**, 1427.
Ryan, C. G., Etschmann, B. E., Vogt, S., Maser, J., Harland, C. L., van Achterbergh, E. & Legnini, D. (2005). *Nucl. Instrum. Methods Phys. Res. B*, **231**, 183–188.
Ryan, C. G. & Jamieson, D. N. (1993). *Nucl. Instrum. Methods Phys. Res. B*, **77**, 203–214.
Ryan, C. G., Kirkham, R., de Jonge, M. D., Siddons, D. P., van der Ent, A., Pages, A., Boesenberg, U., Kuczewski, A., Dunn, P., Jensen, M., Liu, W., Harris, H., Moorhead, G. F., Paterson, D. J., Howard, D. L., Afshar, N., Garrevoet, J., Spiers, K., Falkenberg, G., Woll, A. R., De Geronimo, G., Carini, G. A., James, S. A., Jones, M. W. M., Fisher, L. A. & Pearce, M. (2018). *Synchrotron Radiat. News*, **31**(6), 21–27.
Siddons, D. P., Kirkham, R., Ryan, C. G., De Geronimo, G., Dragone, A., Kuczewski, A. J., Li, Z. Y., Carini, G. A., Pineli, D., Beuttenmuller, R., Elliot, D., Pfeffer, M., Tyson, T. A., Moorhead, G. F. & Dunn, P. A. (2014). *J. Phys. Conf. Ser.* **499**, 012001.
Wilson, S. (2019). Personal communication.